https://doi.org/10.5194/acp-2020-506
Preprint. Discussion started: 6 July 2020
© Author(s) 2020. CC BY 4.0 License.

Atmospheric Chemistry and Physics
Discussions

Effect of NO_X, O_3 and NH_3 on sulfur isotope composition during heterogeneous oxidation of SO_2: a laboratory investigation

Zhaobing Guo[1], Mingyi Xu[1], Yuxuan He[1], Shuo Gao[1], Chenmin Xu[2], Bin Zhu[3], Qingjun Guo[4], Xiaoyu Shen[1], Shuang Zhao[1], Pengxiang Qiu[1]

[1]Jiangsu Key Laboratory of Atmospheric Environment Monitoring and Pollution Control (AEMPC), Collaborative Innovation Center of Atmospheric Environment and Equipment Technology (CIC-AEET), School of Environmental Science and Engineering, Nanjing University of Information Science and Technology, Nanjing 210044, China
[2]School of Environment, Nanjing Normal University, Nanjing 210023, China
[3]School of Atmospheric Physics, Nanjing University of Information Science and Technology, Nanjing 210044, China
[4]Insititude of Geographic Sciences and Natural Resources Research, Chinese Academy of Sciences, Beijing 100101, China

Correspondence to: Chenmin Xu (chenminxu@njnu.edu.cn) and Pengxiang Qiu (pxqiu@nuist.edu.cn)

Abstract. Sulfate aerosol is a major fraction of haze, playing an important role in aerosol formation and aging processes. In order to understand the mechanism of sulfate formations, the characteristics of sulfur isotope composition were determined during different heterogeneous oxidation reactions of sulfur dioxide. Although NH_3 was more beneficial to the formation of sulfate, compared with NO_X and O_3, ^{34}S tended to enrich the lighter sulfur isotopes in the presence of NH_3. Furthermore, in consideration of the potential competitive effects of NO_X, O_3, and NH_3 in the heterogeneous oxidation processes, the contributions of each gas were evaluated via Rayleigh distillation model. Notably, NO_X oxidation contributed 67.5±10 % of the whole sulfate production, which is higher than O_3 (13.3±10 %), and NH_3 oxidation (19.2±10 %) on the basic of the average fractionation factor. The observed $\delta^{34}S$ values of sulfate aerosols were negatively correlated with sulfur oxidation ratios, owing to the sulfur isotopic fractionations during the sulfate formation processes. Given the isotope mass balance, the overall $\delta^{34}S_{sulfate}$ approached the $\delta^{34}S_{emission}$ as oxidation of SO_2 progressed, suggesting that NO_X played a major rather than a sole role in the different heterogeneous oxidation processes of SO_2.

Keywords. Sulfur isotope, oxidation mechanism, fractionation, Rayleigh distillation model

1 Introduction

Haze, a pollution phenomenon that reduces atmospheric visibility to less than 10 km due to the fine particles suspended in the air (Guo et al., 2018; Chen et al., 2019), has aroused widespread concerns in China (Huang et al., 2014; Zhang et al., 2012; DiTucci et al., 2018). The long-term exposure to haze can induce rhinitis and bronchitis, and even lead to lung cancer (Yinon et al., 2017; Wang et al., 2014; Yang et al., 2018). It has been widely recognized that the key factor to the mechanism of haze is the growth of the secondary pollutants and aerosol (Zhang et al., 2019; Zhao et al., 2013; Liu et al., 2012).

Sulfur (S), as an element in sulfate aerosol and various secondary pollutants, is the key to study the formation and evolution of haze. The haze mainly contains sulfur compounds such as H_2S, SO_2, and SO_3, among which sulfur dioxide (SO_2)

https://doi.org/10.5194/acp-2020-506
Preprint. Discussion started: 6 July 2020
© Author(s) 2020. CC BY 4.0 License.

emission from fossil burning is the main source of anthropogenic sulfate aerosol (Haywood et al., 2000). SO_2 can be converted to sulfate via the gas-phase oxidation and heterogeneous reactions (Wang et al., 2019; Kong et al., 2014). Sulfate aerosol not only affects the global climate through direct and indirect radiative forcing (Anderson et al., 2003; Rosenfeld et al., 2014), but also threatens the human respiratory system (Liu et al., 2019). Studying the source and formation mechanism of sulfate aerosol in the atmosphere is of great significance for clarifying the climate change characteristics (Chen et al., 2015). However, the formation mechanism of sulfate is still unclear. Guo et al. (2017) reported that catalytic oxidation of metal ions contributed the most to the formation of sulfate. It was confirmed that SO_2, NO_X, and NH_3 synergistically accelerated the formation of sulfate under high humidity (Wang et al., 2016). Li et al. (2018) demonstrated that the oxidation of S(IV) in haze in China was driven by the $HONO/NO_2^-$ generated due to the consumption of NO_2 on the surface of aerosols. Besides, aqueous NO_2 serves as the dominant oxidant of SO_2 at highly elevated NO_X levels (Xue et al., 2019). Moreover, the synergistic effect between NO_2 and SO_2 on the surface of mineral promotes the conversion of SO_2 to sulfate. Therefore, the oxidation processes of SO_2 cannot be summarized by a simple oxidation mechanism.

The heterogeneous oxidation is the core process of the formation of secondary aerosol, having a guiding role in revealing the formation mechanism of the compound pollution (Lu et al., 2018). The measured sulfur isotopic fractionation showed that about -9 ‰ is for homogeneous oxidation of SO_2 and up to +16.5 ‰ is for heterogeneous oxidation of SO_2 (Chen et al., 2017). In addition, the pathways of SO_2 oxidation in aqueous-phase systems include reactions with O_3, H_2O_2, NO_2, and by O_2 via catalyst (Hung et al., 2015). The formation of sulfate was demonstrated that it was mainly affected by a synergistic effect between NO_X and SO_2 (Gao et al., 2020). Sulfate formations measured during autumn were mainly related to excessive O_2 with Fe^{3+} as catalyst (Guo et al., 2014). Therefore gaseous oxides are the key oxidation pathways in the formation of sulfate during the heterogeneous oxidation process (Chen et al., 2017).

The formation process of the secondary sulfate and sources of sulfur in the atmosphere can be investigated by sulfur isotope ratios (Han et al., 2017), as the characteristics of different sulfur sources can be represented by sulfur isotopic signatures (^{32}S and ^{34}S) (Winterholler et al., 2008). Besides, sulfur isotopes also exhibit distinctive isotope fractionations for different oxidation processes of SO_2 (Han et al., 2016a), which can be applied in the study of formation processes of sulfate. The enrichment of heavy sulfur isotopes in sulfate may be caused by heterogeneous oxidation of SO_2, whereas light sulfur isotopes in sulfate may be attributed to homogeneous oxidation (Chen et al., 2017). Nevertheless, isotope fractionations can only be used to roughly distinguish between the heterogeneous and homogeneous oxidation. The specific oxidation path of SO_2 cannot be discriminated due to the similarity of the sulfur isotope fractionation under different conditions during the oxidation processes of SO_2.

Some investigations about sulfur isotope composition and fractionation have been performed for understanding the formation pathways of sulfate aerosols (Harris et al., 2013b; Yang et al., 2018; Chen et al., 2017). However, most of these observational and modeling studies investigate the sulfur isotope composition in real atmosphere without physical boundaries (Han et al., 2016b; Li et al., 2020). Yet to date, a few experiments were performed in limited physical boundaries to explore the mechanism of sulfur isotope fractionation on the microscale (Harris et al., 2012a; Harris et al., 2012b). To our best knowledge, the effect of NO_X, O_3 and NH_3 on sulfur isotope composition during heterogeneous oxidation of SO_2 have not been determined experimentally. Herein, for the first time, the several SO_2 oxidation processes with different chemical condition (NO_X, O_3 and NH_3) are conducted in laboratory to gain insight into the sulfur isotope fractionation. Furthermore, the sulfur isotopic fractionations were investigated with the Rayleigh distillation model to understand the relative contribution of each SO_2 oxidation pathway. It may not only provide a theoretical basis for the causes of subsequent sulfates, but also be crucial for improving the air quality and studying the regional climate change.

2 Materials and Methods

2.1 Material and methods

Sampling site was located on the roof of the library in Nanjing University of Information Science & Technology (32.1°N, 118.5°E). $PM_{2.5}$ samples were collected by using a high volume sampler (TH-1000H, Tianhong Co., Wuhan) with a flow rate of 1.05 m^3 min^{-1} from 9 am to 9 pm per day from 26th Feb. 2016 to 6th Apr. 2016.

Hematite (α-Fe_2O_3) in the experiments was prepared according to the previous studies (Legodi et al., 2007; Fu et al., 2006). A plate with evenly dispersed α-Fe_2O_3 powder was loaded into the experimental apparatus. On the basis of SO_2-Ar, different proportions of NO_X (O_3 or NH_3) were added to the reactor, combined with/without O_2 and/or light. The NO_X was composed of NO_2 and NO with volume ratio of 2:1. The flow rates of Ar and SO_2 were 95 and 2 mL min^{-1} respectively. The flow rates of NO_X (O_3 or NH_3) varied from 2 to 16 mL min^{-1} depending on the ratio of SO_2 to NO_X (O_3 or NH_3). The wavelength of ultraviolet (UV) light is 303 nm, and the light intensity is 25 $\mu W\ cm^{-2}$. All of the experiments were conducted for 2 h at a temperature of 298 K with a relative humidity of nearly 40 %. The values of temperature and humidity in the experiments were set similarly to those in the air during this period.

The obtained samples were soaked in 50 mL of Milli-Q water and sonicated for 30 minutes to extract sulfate. The samples were centrifuged to separate the sulfate supernatant. The dissolved sulfate in the supernatant was precipitated as $BaSO_4$ by adding 1 mol L^{-1} $BaCl_2$ solution. The $BaSO_4$ precipitates were separated with 0.22 μm acetate membrane and rinsed with 150 mL Milli-Q water to remove Cl^-. The $BaSO_4$ powder was calcined at 1123 K in a muffle furnace for 2 h to obtain the final pure $BaSO_4$ sample.

2.2 Sulfur stable isotope determination

The $\delta^{34}S$ value was determined by using isotope mass spectrometer (IRMS, Delta V Plus, Finningan) and Elemental analyzer (EA, Flash 2000, Thermo). $BaSO_4$ was used as an analytical sample of sulfur isotope composition. The result was with respect to international standard V-CDT, and the accuracy was better than ±0.2 %.

3 Results and discussion

First all, for confirming the sulfur isotope composition and fractionation, $PM_{2.5}$ samples from 26th Feb. to 6th Apr. were collected and the $\delta^{34}S$ values of them were measured. $\delta^{34}S$ value may change when SO_2 is oxidized into the sulfate in the atmosphere via different oxidation pathways. $\delta^{34}S$ aerosol and SO_2 Oxidation Ratio (SOR = $SO_4^{2-}/(SO_4^{2-} + SO_2)$) calculated throughout the sample period were shown in Fig. 1. It can be found that the $\delta^{34}S_{aerosol}$ values showed a ~3.9 ‰ variation, and displayed a negative correlation with SOR. The variation of $\delta^{34}S_{aerosol}$ values was attributed to the isotope fractionation during the oxidation processes of SO_2 (Li et al., 2020). To shed light on the mechanism of SO_2 oxidation in sulfur isotope fractionation and sulfate formation, the SO_2 oxidation processes on the surface of α-Fe_2O_3 in the presence of NO_X, O_3, and NH_3 were carried out in laboratory.

© Author(s) 2020. CC BY 4.0 License.

NO_X is the most important oxidant during the heterogeneous oxidation of SO_2 taking the impact of ion strength into account. As shown in Fig. 2, the yield of SO_4^{2-} ranged from 0.0097 to 0.7795 g and the values of $\delta^{34}S$ were 2.9–4.8 ‰. It was noteworthy that there was an obvious discrepancy between the yield of SO_4^{2-} and the sulfur isotope values. Few sulfates were formed via the heterogeneous reaction between NO_X and SO_2 on the surface of mineral in the dark, whereas the formation of sulfate was enhanced under light, suggesting that UV light could promote the oxidation of SO_2. Besides, in the presence of O_2, NO_X and mineral oxides could act as catalysts to increase the conversion rate of SO_2 on the surface of mineral oxides (Gao et al., 2020). In addition, the increase in the amount of NO_X was another key factor that led to the acceleration of sulfate formation (Cheng et al., 2016). When NO_X and SO_2 coexisted, the content of sulfite on the surface of all oxides was reduced significantly (Pan et al., 2019). Simultaneously, HONO was formed by NO_2 and subsequent hydrolysis in thin films of water coating boundary layer surfaces according to reaction (R1) (Kebede et al., 2016). The release of HONO may help to sustain the efficient sulfate production and droplet acidity. Moreover, the co-adsorption of the oxidant N_2O_4 formed from nitrate under the action of S(IV) further led to the formation of sulfate (Cheng et al., 2016).

$$NO_X + H_2O \rightarrow HONO + HNO_3, \quad (R1)$$

$$NO_2 \xrightarrow{S(IV)} N_2O_4, \quad (R2)$$

$$N_2O_4 + SO_3^{2-} \rightarrow SO_4^{2-} + NO_2^-, \quad (R3)$$

The different proportion of SO_2 and NO_X made a great growth of the sulfur isotope values, which suggested that the $\delta^{34}S$ values were largely dependent on the concentration of NO_X. The sulfur isotope values all reached the maximum when $SO_2 : NO_X$ was 1:8 under different conditions, indicating a significant sulfur isotopic fractionation effects. It was observed that the $\delta^{34}S$ values were relatively lower in the presence of only O_2. It was well-known that the reaction between SO_2 and O_2 was conducted via radical chain reactions in the presence of Fe(III) (Hung et al., 2015), which favored the enrichment of lighter isotopes (Han et al., 2016b). Therefore, under dark conditions, the sulfur isotope value was mainly affected by oxygen and the catalytic action of Fe(III), resulting in the enrichment of lighter sulfur isotopes (Han et al., 2016a). In addition, the $\delta^{34}S$ values of vehicle exhaust from which NO_X emissions were primarily derived were much higher compared to those of coal combustion (Grewling et al., 2019; Guo et al., 2016), indicating that ^{34}S tended to enrich higher sulfur isotopes in the presence of NO_X.

O_3 also exerted an influence on the formation of sulfate and sulfur isotope values. The yield of SO_4^{2-} ranged from 0.0081 to 0.6712 g with the $\delta^{34}S$ values of 1.6–2.9 ‰ (Fig. 3). The rapid growth sulfate yields indicated that the oxidation of SO_2 was sensitive to the concentration of ozone. Ozone, as a very efficient oxidant, could react with the sulfite to release oxygen, promoting the subsequent oxidation of SO_2, which was described as:

$$SO_3^{2-} + O_3 \rightarrow SO_4^{2-} + O_2, \quad (R4)$$

$$HSO_3^- + O_3 \rightarrow HSO_4^- + O_2, \quad (R5)$$

Whether the oxidation processes were on the surface of Fe_2O_3 mineral dust or not, the coexistence of O_3 can convert SO_2 to sulfate (Gao et al., 2020). The highest sulfate production obtained at a ratio of 1:12 may be attributed to the higher photochemical activities and ozone concentration (Kong et al., 2019). Besides, irradiation had been demonstrated to prevent surface saturation for ozone uptake on mineral (Nicoals et al., 2019). These results suggested that experimental conditions, such as ozone and irradiation, changed the quantity of SO_2 taken up and oxidised. Under dark conditions, photolysis of O_3 were negligible, thus surface reactions will be solely responsible for sulfate production (Harris et al., 2013a). Moreover, the

https://doi.org/10.5194/acp-2020-506
Preprint. Discussion started: 6 July 2020
© Author(s) 2020. CC BY 4.0 License.

photolysis of ozone under UV radiation formed electronically excited $O(^1D)$, and its subsequent reaction with water vapor could generate a mass of hydroxyl radicals (Ran et al., 2014; Cheng et al., 2016). As adsorption sites for water, surface hydroxyls were the principal reactive sites on metal oxides. In turn, the adsorbed water was either dissociated into more hydroxyls at oxygen vacancies or hydrogen-bonded to surface O-H groups, which was in favor of the heterogeneous oxidation of SO_2 (Wang et al., 2019).

$$O_3 + h\upsilon \rightarrow O(^1D) + O_2, \quad \text{(R6)}$$

$$O(^1D) + H_2O \rightarrow 2{\bullet}OH, \quad \text{(R7)}$$

$$\bullet OH + SO_2 + M \rightarrow HO_2 + SO_4^{2-}, \quad \text{(R8)}$$

It can be observed from Fig. 3b that the elevation of $\delta^{34}S$ values was related to the concentration of O_3. The oxidation by O_3 dominated in the reaction and favored heavy sulfur isotopes (Han et al., 2016b). The high $\delta^{34}S$ values, especially the highest value obtained at the ratio of 1:8, may be in relation to •OH which promoted the enrichment of heavy sulfur isotopes (Harris et al., 2012b). The values of sulfur isotope in the presence of O_2 were relatively lower than that under the condition of both O_2 and light, indicating that the synergistic effect of O_2 and light facilitated the enrichment of higher sulfur isotope values. In addition, uptake and decomposition of ozone under irradiation increased the basicity of the surface, which was conducive to enrich heavy sulfur isotopes (Hanisch et al., 2003). Harris et al. (2012) confirmed the hypothesis that equilibration to higher pH increased fractionation.

NH_3, as another one of the main pollutants, played an important role in the formation of atmospheric sulfate. It can be observed that the yield of SO_4^{2-} ranged from 0.0237 to 0.9469 g with the $\delta^{34}S$ values of 0.8–4.3 ‰ (Fig. 4). Acidic aerosols can react with gaseous ammonia to form completely or partially neutralized ammonium salts (Donaldson et al., 2010). The extent of aerosol neutralization was determined principally by the ambient concentration of NH_3 and the oxidation rate of SO_2 (Kong et al., 2019). When ammonia was in excess, sulfate aerosol should be mainly presented as ammonium sulfate (Silvern et al., 2017). Herein, the results showed that the reaction of NH_3 with acid may lead to an increase in the formation of sulfate. In addition, surface Lewis basicity might be provided by NH_3 for SO_2 absorption on the mineral, increasing the amount of condensed water on the secondary aerosols and enhancing the formation of sulfate (Chu et al., 2016). Moreover, the oxygen vacancies in α-Fe_2O_3 may lead to the formation of sulfate on α-Fe_2O_3 (Wang et al., 2019).

Of note, the effect of NH_3 on the sulfur isotope composition was not apparent with the relatively stable overall trend. Under only-light, NH_3, which increased the alkalinity by producing OH^- from hydrolysis, dominated in the reaction, leading to an increase of $\delta^{34}S$ values (Jiang et al., 2017). O_2 with Fe^{3+} as catalyst dominant in the presence of only-oxygen favored light sulfur isotopes, which was consistent with above results. The $\delta^{34}S$ values of sulfate increased with the increases of sulfate concentrations under the combined oxygen with light (Doi et al., 2004). Therefore, we inferred that O_2 and light had a synergistic effect on the sulfur isotope compositions in the presence of NH_3. Compared with the $\delta^{34}S$ values in the presence of NO_X above, S under NH_3 was more inclined to enrich the lighter sulfur isotopes. The $\delta^{34}S$ values from main biogenic source of NH_3 were on the low side, indicating that the effects of NH_3 on sulfur isotopic compositions were relatively mild (Han et al., 2016a; Grewling et al., 2019). Simultaneously, there was only a slight fluctuation of the $\delta^{34}S$ values with the rapidly increasing of the sulfate production in the presence of O_2 and light. Hence, the existence of NH_3 increased the conversion rate of SO_2 and the sulfate production with little effects on the isotope fractionation.

To make clear the relative contribution of NO_X, O_3, and NH_3, we investigated the isotope fractionation of sulfate. The

© Author(s) 2020. CC BY 4.0 License.

oxidation of SO_2 to sulfate caused the fractionation of isotope ratios as long as the reaction is not complete. Isotope fractionation is divided into equilibrium and kinetic fractionation. The coefficient α considered as the kinetic rate constants ratio can represent the fractionation effects. When the reactant is presented as an infinite reservoir and not affected by the reaction, α_{34} can be calculated from the isotopic compositions of reactants and products (Harris et al., 2012a):

$$\alpha_{34} = \frac{R_{\text{products}}}{R_{\text{reactants}}}, \tag{1}$$

Among them, $R={}^{34}S/{}^{32}S$. Thus, $\alpha > 1$ indicates that the reactions are more inclined to enrich heavy isotopes.

The $\delta^{34}S$ value of SO_2 sources ($\delta^{34}S_{\text{emission}}$) strongly depends on the origin of SO_2, thus it is difficult to constrain (Li et al., 2018). On the basis of the literature, +2.7±2.0 ‰ is used as the $\delta^{34}S_{\text{emission}}$ value during our sampling period (Li et al., 2020). Therefore, we used a Rayleigh distillation model and the isotopic enrichment factor ($\varepsilon = (\alpha-1)*1000‰$) to explain the discrepancy between $\delta^{34}S$ and $\delta^{34}S_{\text{emission}}$ values and quantify the contributions of each oxidant on the basis of the above results in the experiment. The fractionation factor is found from the Rayleigh equation describing the $\delta^{34}S_{\text{sulfate}}$ with respect to the fraction of oxidized SO_2 (Harris et al., 2012a):

$$\alpha_{34} = \frac{\ln(1-(\frac{R_p}{R_i})(1-f))}{\ln f}, \tag{2}$$

Where R_p and R_i are the ratios of ${}^{34}S/{}^{32}S$ for the product sulfate and the initial SO_2 gas respectively and f (1-SOR) is the fraction of remaining SO_2.

The measured ε_{obs} values as a result of mixing oxidation pathways of $SO_2 + NO_X + O_3 + NH_3$ were +1.3±1.4 ‰ by simulations (Fig. 5). NO_X oxidation enriched ${}^{34}S$ in the product sulfate with an enrichment factor (ε_{NOX}) of +2.1 ‰, and oxidation by O_3 pathway depleted ${}^{34}S$ (ε_{O_3}=+0.2 ‰) in the product sulfate, and oxidation by NH_3 pathway enriched ${}^{34}S$ in the product sulfate with a ε_{NH3} value of -0.6 ‰. Considering the isotope mass balance, the overall ε_{obs} value (+1.3 ‰) fell in between NOx, O_3, and NH_3 values and approached $\delta^{34}S_{\text{emission}}$ as oxidation of SO_2 progressed, indicating that NO_X, O_3, and NH_3 all had a certain influence on the heterogeneous oxidation of SO_2.

$$\varepsilon_{\text{obs}} = \varepsilon_{NOx} * f_{NOx} + \varepsilon_{O_3} * f_{O_3} + \varepsilon_{NH_3} * f_{NH_3}, \tag{3}$$

In which ε and f are the enrichment factor and the contribution of different pathways respectively, and $f_{NOx} + f_{O_3} + f_{NH_3} = 1$.

Using the Eq. 3, we determined the overall contributions from NOx, O_3, and NH_3 pathways were 67.5±10 %, 13.3±10 %, 19.2±10 %, respectively. During the period of collecting $PM_{2.5}$, the average concentration of NO_X and O_3 showed a negative correlation, and the overall concentration of NO_X in the atmosphere was lower than that of O_3. However, NO_X accounted for a larger proportion in sulfur isotope fractionation due to its tendency to enrich heavier sulfur, suggesting the NO_X pathway have played a more important role during the oxidation of SO_2.

4 Conclusion

NO_X exerted a driving influence on the enrichment of heavy sulfur isotopes. Hydroxyl radical formed by the photolysis of O_3 favored the enrichment of relatively heavy sulfur isotopes. Although NH_3 was more conducive to the formation of sulfate compared with NO_X and O_3, there existed lighter sulfur isotopes with a slight effect on the isotope fractionation in the presence of NH_3. The evaluated contributions of NO_X, O_3, and NH_3 oxidations were 67.5±10 %, 13.3±10 %, and 19.2±10 % respectively via the Rayleigh distillation model and average fractionation factor. On the basis of the isotope mass balance, we concluded that NO_X pathway was a dominating but not sole pathway during different heterogeneous oxidation processes of SO_2, which laid the foundation for the research of the mechanism of sulfate formation.

Author contribution.

ZBG designed the methodology, administrated the project and wrote the original draft. MYX performed model simulations and analyzed the data. YXH conducted the investigation process. SG provided the study materials. XYS performed the data collection. SZ provided the laboratory samples. BZ, QJG and CMX wrote the review and commentary. PXQ reviewed and revised the paper.

Acknowledgment

We gratefully acknowledge the financial supports from the National Natural Science Foundation of China (Nos. 41873016, 51908293, 51908294 and 41625006), National key R&D program of China (91544229-02), Jiangsu Province 333 Talent Project (BRA2018033) and the Natural Science Foundation of Jiangsu Province (BK20190718).

Competing interests. The authors declare that they have no conflict of interest.

References

Anderson, T. L. and Charlson, R. J.: Climate Forcing by Aerosols-A hazy picture, Science., 300 (5622), 1103 – 1104, doi:10.2307/3834024, 2003.

Yang, D. A., Bardoux, G., Assayag, N., Laskar, C., Widory, D., and Cartigny, P.: Atmospheric SO_2 oxidation by NO_2 plays no role in the mass independent sulfur isotope fractionation of urban aerosols, Atmos. Res., doi:10.1016/j.atmosenv.2018.09.007, 2018.

Chen, S. L., Guo, Z. Y., Guo, Z. B., Guo, Q. J., Zhang, Y. L., Zhu, B., and Zhang, H. X.: Sulfur isotopic fractionation and its implication: Sulfate formation in $PM_{2.5}$ and coal combustion under different conditions, Atmos. Res., 194, 142–149, doi:10.1016/j.atmosres.2017.04.034, 2017.

Chen, S., Xu, L., Zhang, Y., Chen, B., Wang, X., Zhang, X., Zhen, M., Chen, J., Wang, W., Sun, Y., Fu, P., Wang, Z., and Li, W.: Direct observations of organic aerosols in common wintertime hazes in North China: insights into direct emissions from Chinese residential stoves, Atmos. Chem. Phys., 17 (2), 1259–1270, doi:10.5194/acp-17-1259-2017, 2017.

Chen, H., Cheng, T., Gu, X., and Wu, Y.: Characterization of aerosols in Beijing during severe aerosol loadings, Atmos. Environ., 119, 273–281, doi:10.1016/j.atmosenv.2015.08.045, 2015.

Chen, H. M., Zhuang, B., Liu, J., Wang, T., Li, S., Xie, M., Li, M., Chen, P., and Zhao, M.: Characteristics of ozone and particles in the near-surface atmosphere in the urban area of the Yangtze River Delta, China, Atmos. Chem. Phys., 19 (7), 4153–4175, doi:10.5194/acp-19-4153-2019, 2019.

Cheng, Y., Yan, L., Huang, Y., Wang, Q., Morawska, L., Gu, Z. L., Cao, J. J., Zhang, L. Y., Li, B. W., and Wang, Y.: Characterization of particle size distributions during winter haze episodes in urban air, Atmos. Res., doi:10.1016/j.atmosres.2019.04.033, 2019.

Cheng, Y. F., Zheng, G., Wei, C., Cheng, Y., Zheng, G., Wei, C., Mu, Q., Zheng, B., Wang, Z., Gao, M., Zhang, Q., He, K., Carmichael, G., Pöschl, U., and Su, H.: Reactive nitrogen chemistry in aerosol water as a source of sulfate during haze events in China, Sci. Adv., 2 (12), e1601530-e1601530, doi:10.1126/sciadv.1601530, 2016.

Chu, B., Zhang, X., Liu, Y., He, H., Sun, Y., Jiang, J., Li, J., and Hao, J.: Synergetic formation of secondary inorganic and organic aerosol: effect of SO_2 and NH_3 on particle formation and growth, Atmos. Chem. Phys., 16 (22), 14219–14230, doi:10.5194/acp-16-14219-2016, 2016.

DiTucci, M. J., Stachl, C. N., and Williams, E. R.: Long distance ion-water interactions in aqueous sulfate nanodrops persist to ambient temperatures in the upper atmosphere, Chem. Sci., 9 (16), 3970–3977, doi:10.1039/c8sc00854j, 2018.

Ding, T., Valkiers, S., Kipphardt, H., Bièvre, P. D., Taylor, P. D. P., Gonfiantini, R., and Krouse, R.: Calibrated sulfur isotope abundance ratios of three IAEA sulfur isotope reference materials and V-CDT with a reassessment of the atomic weight of sulfur, Geochim. Cosmochim. Acta., 65 (15), 2433–2437, doi:10.1016/s0016-7037(01)00611-1, 2001.

Doi, H., Kikuchi, E., Mizota, C., Satoh, N., Shikano, S., Yurlova, N., Yadrenkina, E., and Zuykova, E.: Carbon, nitrogen, and sulfur isotope changes and hydro-geological processes in a saline lake chain, Hydrobiologia., 529 (1), 227–237, doi:10.1007/s10750-004-6418-2, 2004.

Donaldson, D. J. and Valsaraj, K. T.: Adsorption and Reaction of Trace Gas-Phase Organic Compounds on Atmospheric Water Film Surfaces: A Critical Review, Environ. Sci. Technol., 44 (3), 865–873, doi:10.1021/es902720s, 2010.

Fu, H. and Quan, X.: Complexes of fulvic acid on the surface of hematite, goethite, and akaganeite: FTIR observation, Chemosphere., 63 (3), 403–410, doi:10.1016/j.chemosphere.2005.08.054, 2006.

Gao, M., Liu, Z., Zheng, B., Ji, D., Sherman, P., Song, S., Xin, J., Liu, C., Wang, Y., Zhang, Q., Xin, J., Jiang, J., Wang, Z., Carmichael, G. R., and McElroy, M. B.: China's emission control strategies have suppressed unfavorable influences of climate on wintertime $PM_{2.5}$ concentrations in Beijing since 2002, Atmos. Chem. Phys., 20 (3), 1497–1505, doi:10.5194/acp-20-1497-2020, 2020.

Gao, M., Carmichael, G. R., Wang, Y., Ji, D., Liu, Z., and Wang, Z.: Improving simulations of sulfate aerosols during winter haze over Northern China: the impacts of heterogeneous oxidation by NO_2, Front. Environ. Sci. Eng., 10(5), doi:10.1007/s11783-016-0878-2, 2016.

Ge, S., Wang, G., Zhang, S., Li, D., Xie, Y., Wu, C., Yuan, Q., Chen, J., and Zhang, H.: Abundant NH_3 in China enhances atmospheric HONO production by promoting the heterogeneous reaction of SO_2 with NO_2, Environ. Sci. Technol., doi:10.1021/acs.est.9b04196, 2019.

Grewling, Ł., Bogawski, P., Kryza, M., Magyar, D., Sikoparija, B., Skjoth, C. A., Udvardy, U., Werner, M., and Smith, M.: Concomitant occurrence of anthropogenic air pollutants, mineral dust and fungal spores during long-distance transport of ragweed pollen, Environ. Pollut., doi:10.1016/j.envpol.2019.07.116, 2019.

© Author(s) 2020. CC BY 4.0 License.

Guo, Z. Y., Guo, Q. J., Chen, S. L., Zhu, B., Zhang, Y. L., Yu, J. H., and Guo, Z. B.: Study on pollution behavior and sulfate formation during the typical haze event in Nanjing with water soluble inorganic ions and sulfur isotopes, Atmos. Res., doi:10.1016/j.atmosres.2018.11.009, 2018.

Guo, Z. B, Shi, L., Chen, S. L., Jiang, W., Wei, Y., Rui, M. L., and Zeng, G.: Sulfur isotopic fractionation and source appointment of $PM_{2.5}$ in Nanjing region around the second session of the Youth Olympic Games, Atmos. Res., 174–175, doi:10.1016/j.atmosres.2016.01.011, 2016.

Guo, H., Weber, R. J., and Nenes, A.: High levels of ammonia do not raise fine particle pH sufficiently to yield nitrogen oxide-dominated sulfate production, Sci. Rep., 7 (1), doi:10.1038/s41598-017-11704-0, 2017.

Haywood, J., and Boucher, O.: Estimates of the direct and indirect radiative forcing due to tropospheric aerosols: A review, Rev. Geophys., 38 (4), 513–543, doi:10.1029/1999rg000078, 2000.

Han, X., Guo, Q., Liu, C., Fu, P., Strauss, H., Yang, J., Hu, J., Wei, L., Ren, H., Peters, M., Wei, R., and Tian, L.: Using stable isotopes to trace sources and formation processes of sulfate aerosols from Beijing, China, Sci. Rep., 6 (1), doi:10.1038/srep29958, 2016a.

Han, X., Guo, Q., Liu, C., Strauss, H., Yang, J., Hu, J., Wei, R., Tian, L., Kong, J., and Peters, M.: Effect of the pollution control measures on $PM_{2.5}$ during the 2015 China Victory Day Parade: Implication from water-soluble ions and sulfur isotope, Environ. Pollut., 218, 230–241, doi:10.1016/j.envpol.2016.06.038, 2016b.

Han, X., Guo, Q., Strauss, H., Liu, C., Hu, J., Guo, Z., Wei, R., Peters, M., Tian, L., and Kong, J.: Multiple Sulfur Isotope Constraints on Sources and Formation Processes of Sulfate in Beijing $PM_{2.5}$ Aerosol, Environ. Sci. Technol., 51 (14), 7794–7803, doi:10.1021/acs.est.7b00280, 2017.

Hanisch, F. and Crowley, J. N.: Ozone decomposition on Saharan dust: an experimental Investigation, Atmos. Chem. Phys., 3, 119–130, doi:10.5194/acp-3-119-2003, 2003.

Harris, E., Sinha, B., Foley, S., Crowley, J. N., Borrmann, S., and Hoppe, P.: Sulfur isotope fractionation during heterogeneous oxidation of SO_2 on mineral dust, Atmos. Chem. Phys., 12, 4867–4884, doi:10.5194/acp-12-4867-2012, 2012a.

Harris, E., Sinha, B., Hoppe, P., Crowley, J. N., Ono, S., and Foley, S.: Sulfur isotope fractionation during oxidation of sulfur dioxide: gas-phase oxidation by OH radicals and aqueous oxidation by H_2O_2, O_3 and iron catalysis, Atmos. Chem. Phys., 12, 407–424, doi:10.5194/acp-12-407-2012, 2012b.

Harris, E., Sinha, B., Pinxteren, D. V., Tilgner, A., Fomba, K. W., Schneider, J., Roth, A., Gnauk, T., Fahlbusch, B., Mertes, S., Lee, T., Collett, J., Foley, S., Borrmann, S., Hoppe, P., and Herrmann, H.: Enhanced role of transition metal ion catalysis during in-cloud oxidation of SO_2, Science., 340, 727–730, doi:10.1126/science.1230911, 2013a.

Harris, E., Sinha, B., Hoppe, P., and Ono, S.: High-Precision Measurements of ^{33}S and ^{34}S Fractionation during SO_2 Oxidation Reveal Causes of Seasonality in SO_2 and Sulfate Isotopic Composition, Environ. Sci. Technol., 47 (21), 12174–12183, doi:10.1021/es402824c, 2013b.

Huang, R., Zhang, Y., Bozzetti, C., Ho, K., Cao, J., Han, Y., Daellenbach, K. R., Slowik, J. G., Platt, S. M., Canonaco, F., Zotter, P., Wolf, R., Pieber, S. M., Bruns, E. A., Crippa, M., Ciarelli, G., Piazzalunga, A., Schwikowski, M., Abbaszade, G., Kreis, J. S., Zimmermann, R., An, Z., Szidat, S., Baltensperger, U., Haddad, I. E., and Prévôt, A. S. H.:

High secondary aerosol contribution to particulate pollution during haze events in China, Nature., 514, 218–222, doi:10.1038/nature13774, 2014.

Hung, H. M. and Hoffmann, M. R.: Oxidation of Gas-Phase SO_2 on the Surfaces of Acidic Microdroplets: Implications for Sulfate and Sulfate Radical Anion Formation in the Atmospheric Liquid Phase, Environ. Sci. Technol., 49 (23), 13768–13776, doi:10.1021/acs.est.5b01658, 2015.

Jiang, B. and Xia, D.: Role identification of NH_3 in atmospheric secondary new particle formation in haze occurrence of China, Atmos. Environ., 163, 107–117, doi:10.1016/j.atmosenv.2017.05.035, 2017.

Kebede, M. A., Bish, D. L., Losovyj, Y., Engelhard, M. H., and Raff, J. D.: The Role of Iron-Bearing Minerals in NO_2 to HONO Conversion on Soil Surfaces, Environ. Sci. Technol., 50 (16), 8649–8660, doi:10.1021/acs.est.6b01915, 2016.

Kong, L. D, Zhao, X., Sun, Z. Y., Yang, Y. W., Fu, H. B., Zhang, S. C., Cheng, T. T., Yang, X., Wang, L., and Chen, J. M.: The effects of nitrate on the heterogeneous uptake of sulfur dioxide on hematite, Atmos. Chem. Phys., 14 (17), 9451–9467, doi:10.5194/acp-14-9451-2014, 2014.

Kong, L., Tang, X., Zhu, J., Wang, Z., Fu, J. S., Wang, X., Itahashi, S., Yamaji, K., Nagashima, T., Lee, H. L., Kim, C. H., Lin, C. H., Chen, L., Zhang, M., Tao, Z., Li, J., Kajino, M., Liao, H., Sudo, K., Wang, Y., Pan, Y., Tang, G., Li, M., Wu, Q., Ge, B., and Carmichael, G. R.: Evaluation and uncertainty investigation of the NO_2, CO and NH_3 modeling over China under the framework of MICS-Asia III, Atmos. Chem. Phys. Discuss., 1–33, doi:10.5194/acp-2018-1158, 2019.

Legodi, M. and Dewaal, D.: The preparation of magnetite, goethite, hematite and maghemite of pigment quality from mill scale iron waste, Dyes. Pigments., 74 (1), 161–168, doi:10.1016/j.dyepig.2006.01.038, 2007.

Li, R., Wang, Z., Cui, L., Fu, H., Zhang, L., Kong, L., Chen, W., and Chen, J.: Air pollution characteristics in China during 2015-2016: Spatiotemporal variations and key meteorological factors, Sci. Total. Environ., 648, 902–915, doi:10.1016/j.scitotenv.2018.08.181, 2019.

Li, J., Michalski, G., Davy, P.; Harvey, M., Katzman, T., and Wilkins, B.: Investigating Source Contributions of Size-Aggregated Aerosols Collected in Southern Ocean and Baring Head, New Zealand Using Sulfur Isotopes, Geophys. Res. Lett., 45 (8), 3717–3727, doi:10.1002/2018gl077353, 2018.

Li, J., Zhang, Y., Cao, F., Zhang, W., Fan, M., Lee, X., and Michalski, G.: Stable Sulfur Isotopes Revealed a Major Role of Transition-Metal-Ion Catalyzed SO_2 Oxidation in Haze Episodes, Environ. Sci. Technol., doi:10.1021/acs.est.9b07150, 2020.

Li, L., Hoffmann, M. R., and Colussi, A. J.: Role of Nitrogen Dioxide in the Production of Sulfate during Chinese Haze-Aerosol Episodes, Environ. Sci. Technol., 52 (5), 2686–2693, doi:10.1021/acs.est.7b05222, 2018.

Liu, X., Li, J., Qu, Y., Han, T., Hou, L., Gu, J., Chen, C., Yang, Y., Liu, X., Yang, T., Zhang, Y., Tian, H., and Hu, M.: Formation and evolution mechanism of regional haze: a case study in the megacity Beijing, China, Atmos. Chem. Phys., 13, 4501–4514, doi:10.5194/acpd-12-16259-2012, 2012.

Lu, K., Guo, S., Tan, Z., Wang, H., Shang, D., Liu, Y., Li, X., Wu, Z., Hu, M., and Zhang, Y.: Exploring atmospheric free-radical chemistry in China: the self-cleansing capacity and the formation of secondary air pollution, Natl. Sci. Rev., doi/10.1093/nsr/nwy073, 2018.

Ma, S., Chai, J., Jiao, K., Ma, L., Zhu, S., and Wu, K.: Environmental influence and countermeasures for high humidity flue gas discharging from power plants, Renew. Sust. Energ. Rev., 73, 225–235, doi:10.1016/j.rser.2017.01.143, 2017.

Ma, J., Chu, B., Liu, J., Liu, Y., Zhang, H., and He, H.: NO_X promotion of SO_2 conversion to sulfate: An important mechanism for the occurrence of heavy haze during winter in Beijing, Environ. Pollut., 233, 662–669, doi:10.1016/j.envpol.2017.10.103, 2018.

Nicolas, M., Ndour, M., Ka, O., D'Anna, B., and George, C.: Photochemistry of Atmospheric Dust: Ozone Decomposition on Illuminated Titanium Dioxide, Environ. Sci. Technol., 43 (19), 7437–7442, 7442, doi:10.1021/es901569d, 2009.

Pan, X., Ge, B., Wang, Z., Tian, Y., Liu, H., Wei, L., Yue, S., Uno, I., Kobayashi, H., Nishizawa, T., Shimizu, A., Fu, P., and Wang, Z.: Synergistic effect of water-soluble species and relative humidity on morphological changes in aerosol particles in the Beijing megacity during severe pollution episodes, Atmos. Chem. Phys., 19 (1), 219–232, doi:10.5194/acp-19-219-2019, 2019.

Pandis, S. N. and Seinfeld, J. H.: Sensitivity analysis of a chemical mechanism for aqueous-phase atmospheric chemistry, J. Geophys. Res., 94 (D1), 1105, doi:10.1029/jd094id01p01105, 1989.

Ran, L., Lin, W., Deji, Y., La, B., Tsering, P. M., Xu, X., and Wang, W.: Surface gas pollutants in Lhasa, a highland city of Tibet-current levels and pollution implications, Atmos. Chem. Phys., 14 (19), 10721–10730, doi:10.5194/acp-14-10721-2014, 2014.

Robinson, E. S., Shah, R. U., Messier, K., Gu, P., Li, H. Z., Apte, J. S., Robinson, A. L., and Presto, A. A.: Land-Use Regression Modeling of Source-Resolved Fine Particulate Matter Components from Mobile Sampling, Environ. Sci. Technol., doi:10.1021/acs.est.9b01897, 2019.

Rosenfeld, D., Sherwood, S., Wood, R., and Donner, L.: Climate Effects of Aerosol-Cloud Interactions, Science., 343 (6169), 379–380, doi:10.1126/science.1247490, 2014.

Silvern, R. F., Jacob, D. J., Kim, P. S., Marais, E. A., Turner, J. R., Campuzano-Jost, P., and Jimenez, J. L.: Inconsistency of ammonium-sulfate aerosol ratios with thermodynamic models in the eastern US: a possible role of organic aerosol, Atmos. Chem. Phys., 17 (8), 5107–5118, doi:10.5194/acp-17-5107-2017, 2017.

Wang, G., Zhang, R., Gomez, M., Yang, L., Zamora, M., Hu, M., Lin, Y., Peng, J., Guo, S., Meng, J., Li, J., Cheng, C., Hu, T., Ren, Y., Wang, Y., Gao, J., Cao, J., An, Z., Zhou, W., Li, G., Wang, J., Tian, P., Marrero-Ortiz, W., Secrest, J., Du, Z., Zheng, J., Shang, D., Zeng, L., Shao, M., Wang, W., Huang, Y., Wang, Y., Zhu, Y., Li, Y., Hu, J., Pan, B., Cai, L., Cheng, Y., Ji, Y., Zhang, F., Rosenfeld, D., Liss, P., Duce, R., Kolb, C., and Molina, M.: Persistent sulfate formation from London Fog to Chinese haze, P. Natl. Acad. Sci. USA., doi:10.1073/pnas.1616540113, 2016.

Wang, Y., Zhang, R. Y., and Saravanan, R.: Asian pollution climatically modulates midlatitude cyclones following hierarchical modeling and observational analysis, Nat. Commun., 5 (1), doi:10.1038/ncomms4098, 2014.

Wang, Z., Wang, T., Fu, H., Zhang, L., Tang, M., George, C., Grassian, V. H., and Chen, J.: Enhanced heterogeneous uptake of sulfur dioxide on mineral particles through modification of iron speciation during simulated cloud processing, Atmos. Chem. Phys. Discuss., 19 (19), 12569–12585, doi:10.5194/acp-2019-435, 2019.

Winterholler, B., Hoppe, P., Huth, J., Foley, S., and Andreae, M. O.: Sulfur isotope analyses of individual aerosol particles in the urban aerosol at a central European site (Mainz, Germany), Atmos. Chem. Phys., 8 (23), 11–36, 7238, doi:10.5194/acp-8-7217-2008, 2008.

Xue, J., Yu, X., Yuan, Z. B., Griffith, S. M., Stephen, M., Lan, A. K. H., Seinfeld, J. H., Yu, J. Z.: Efficient control of atmospheric sulfate production based on three formation regimes, Nat. Geosci., doi:10.1038/s41561-019-0485-5, 2019.

Yang, J. and Zhang, B.: Air pollution and healthcare expenditure: Implication for the benefit of air pollution control in China, Environ. Int., 120, 443–455, doi:10.1016/j.envint.2018.08.011, 2018.

Yinon, L. and Thurston, G.: An evaluation of the health benefits achieved at the time of an air quality intervention in three Israeli cities, Environ. Int., 102, 66–73, doi:10.1016/j.envint.2016.12.025, 2017.

Zhao, D., Zhu, T., Chen, Q., Liu, Y., and Zhang, Z.: Raman micro-spectrometry as a technique for investigating heterogeneous reactions on individual atmospheric particles, Sci. China. Chem., 54 (1), 154–160, 160, doi:10.1007/s11426-010-4182-x, 2011.

Zhang, Q., He, K. B., and Huo, H.: Cleaning China's air, Nature., 484, 161–162, doi:10.1038/484161a, 2012.

Zhang, T., Li, X., Wang, M., Chen, H., and Yao, M.: Microbial aerosol chemistry characteristics in highly polluted air, Sci. China. Chem., doi:10.1007/s11426-019-9488-3, 2019.

Zhao, X. J., Zhao, P. S., Xu, J., Meng, W., Pu, W. W., Dong, F., He, D., and Shi, Q. F.: Analysis of a winter regional haze event and its formation mechanism in the North China Plain, Atmos. Chem. Phys., 13 (11), 5685–5696, doi:10.5194/acp-13-5685-2013, 2013.

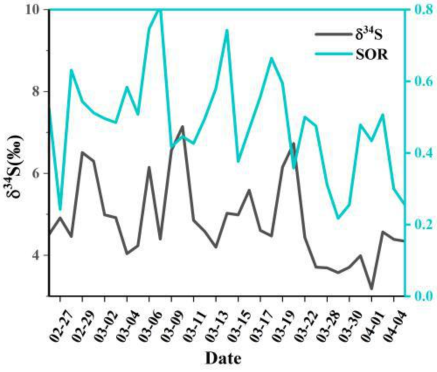

Figure 1: $\delta^{34}S_{aerosol}$ (black), calculated sulfur oxidation ratio (SOR, green) throughout the sample period.

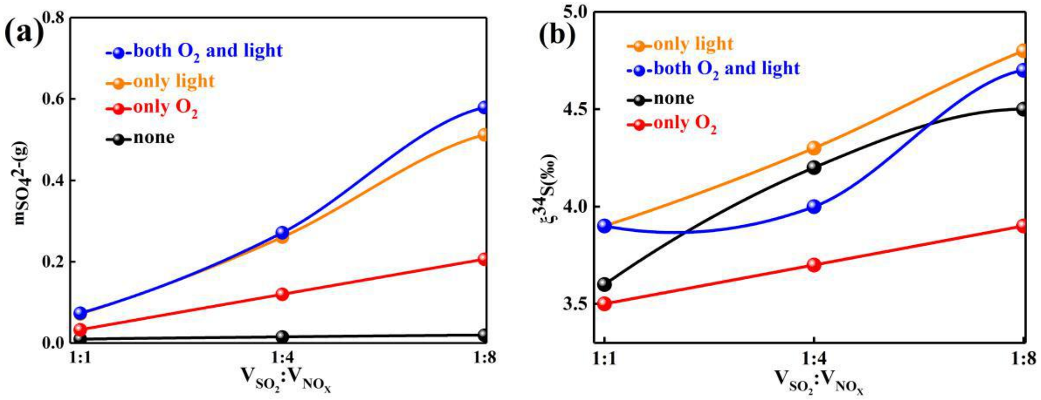

Figure 2: Effect of mixed gas of SO_2 and NO_X on (a) sulfate production and (b) sulfur isotope value under different reaction conditions.

© Author(s) 2020. CC BY 4.0 License.

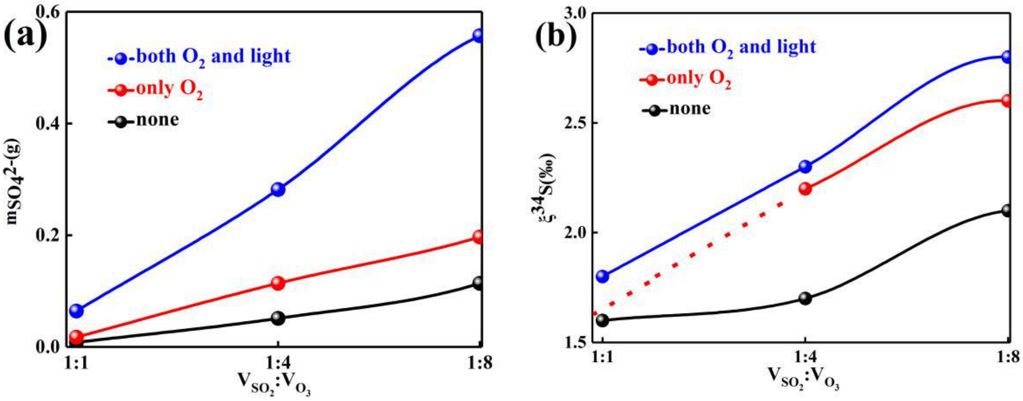

Figure 3: Effect of mixed gas of SO_2 and O_3 on (a) sulfate production and (b) sulfur isotope values under different reaction conditions. (The dotted line represents the trend as it should be).

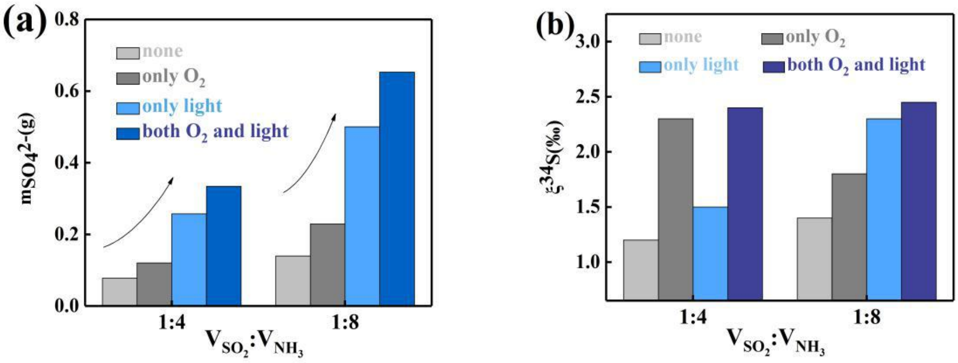

Figure 4: Effect of mixed gas of SO_2 and NH_3 on (a) sulfate production and (b) sulfur isotope values under different reaction conditions.

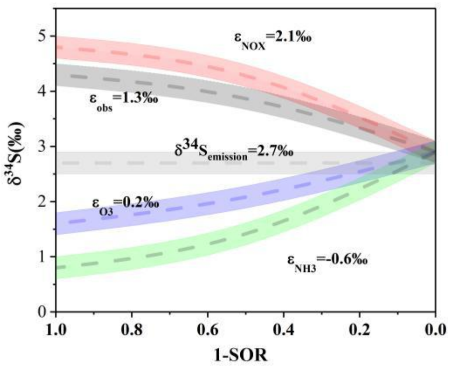

https://doi.org/10.5194/acp-2020-506
Preprint. Discussion started: 6 July 2020
© Author(s) 2020. CC BY 4.0 License.

405 **Figure 5:** Rayleigh distillation model of sulfate production. Grey bar indicates the $\delta^{34}S_{emission}$ (+2.7±2 ‰) in Nanjing. Dashed lines with shaded areas are $\delta^{34}S_{sulfate}$ values: red line indicates the $\delta^{34}S_{sulfate}$ when SO_2 is oxidized solely by NO_X, blue line indicates the $\delta^{34}S_{sulfate}$ when SO_2 is oxidized solely by O_3, green line indicates the $\delta^{34}S_{sulfate}$ when SO_2 is oxidized solely by NH_3, and dark grey line is the ε_{obs} of +1.3 ‰.